

# The Rashba splitting in SmB<sub>6</sub>

O. Rader<sup>1</sup>, P. Hlawenka<sup>1</sup>, K. Siemensmeyer<sup>1</sup>, E. Weschke<sup>1</sup>, A. Varykhalov<sup>1</sup>, J. Sánchez-Barriga<sup>1,2</sup>, N. Y. Shitsevalova<sup>3</sup>, V. B. Filipov<sup>3</sup>, S. Gabáni<sup>4</sup>, K. Flachbart<sup>4</sup>, E. D. L. Rienks<sup>1</sup>

<sup>1</sup>Helmholtz-Zentrum Berlin für Materialien und Energie, Albert-Einstein-Str. 15, 12489 Berlin, Germany

<sup>2</sup>IMDEA Nanoscience, C. Faraday 9, Campus de Cantoblanco, 28049, Madrid, Spain

<sup>3</sup>Institute for Problems of Materials Science, National Academy of Sciences of Ukraine, Krzhyzhanovsky str. 3, Kiev 03142, Ukraine

<sup>4</sup>Institute of Experimental Physics, Slovak Academy of Sciences, Watsonova 47, 04001 Košice, Slovakia

E-mail: rader@helmholtz-berlin.de

## Abstract:

**The present article highlights two aspects at the intersection between Rashba physics and topological matter. Topologically nontrivial matter has been in the focus for almost two decades. It depends strongly on spin-orbit coupling but, in contrast to large parts of modern solid state physics, strong electron correlation does not play a major role. In this context, SmB<sub>6</sub> has been suggested as the first topological insulator driven by strong electron correlation and the first topological Kondo insulator. We review the important role of the Rashba splitting in determining that the observed surface states are not topological. Moreover, we point out that the Rashba splitting of SmB<sub>6</sub> represents the extreme case of a large splitting in momentum space at a small Rashba parameter.**

After incredible hardships and hindrances which can be followed in his memories along with unexpected twists and fortunate coincidences (1), Emmanuel Rashba succeeded in 1954 to join the semiconductor department of the Academy of Sciences in Kiev, which is also

his birthplace. In 1959, he noted together with his student Sheika that spin-orbit interaction creates a spin splitting and spin polarization in the presence of an electrical potential that breaks inversion symmetry. They discovered that in the inversion asymmetric wurtzite structure the spin splitting perpendicular to the  $c$  axis is linear in wave vector  $k$  causing a ring of extrema in the band dispersion  $E(k)$  (2), in contrast to the spin-orbit splitting cubic in  $k$  described by Dresselhaus (3). Later on, the work has been extended to quasi two-dimensional systems (4). The development of the scientific field established by these discoveries has been documented in reviews and focus issues (5-7).

In recent years, a particular consequence of spin-orbit coupling has come into focus, namely topologically nontrivial matter (8,9). Topological insulators are characterized by a non-trivial symmetry-protected topological order characterized by  $Z_2$  invariants which leads to symmetry protected surface states. These surface states appear as Dirac cones with a unique helical spin texture. The bulk band structure features an inverted energy gap in which the linear dispersion of the surface states provides the surface metallicity. Key aspects were already proposed as early as 1985 (10). The spin is locked to the linear momentum which leads in 2D topological insulators to the quantum spin Hall (11) and the quantum anomalous Hall effect (12) where backscattering is forbidden and conductance is quantized. For 3D topological insulators, the presence of topological surface states can directly be verified by angle-resolved photoelectron spectroscopy (ARPES) with and without spin resolution and the predictions from the  $Z_2$  invariants ( $\nu_0; \nu_1, \nu_2, \nu_3$ ) be checked in this way. The strong topological insulator has an odd number of Dirac cone surface states per surface Brillouin zone ( $\nu_0 = 1$ ), distinguishing strong topological materials from topologically weak or trivial materials ( $\nu_0 = 0$ ).

There are several important aspects at the intersection between the Rashba effect and topological insulators. First of all, spin-momentum locking leads to a spin texture that Rashba-type surface states have in common with Dirac-type topological surface states (5,6)

and can be verified by spin-resolved ARPES. Secondly, the topological insulator was at first predicted for graphene under the presence of a sizeable intrinsic spin-orbit interaction (13). The enhancement of a formally intrinsic spin-orbit interaction in a two-dimensional material by external influence is possible but difficult to realize because the creation of a Rashba-type spin-orbit interaction is also likely in this geometry (14). Intercalation of an atomic layer of Au leads indeed to the observation of a giant Rashba splitting in the Dirac cone of graphene (15). In the present article, we would like to address two additional important aspects both of which have to do with the properties of  $\text{SmB}_6$ . The first one concerns the controversial question whether or not  $\text{SmB}_6$  is the first strongly correlated topological insulator, and the second one highlights the properties of surface states with 4f character.

Topological insulators are defined via their single-particle band structure and do not depend on electron correlation, in contrast to effects such as unconventional superconductivity, metal-to-insulator transitions, or the Kondo effect. In this context, it is also worthwhile to note that topological insulators constitute an exotic phase of matter not described by the concept of spontaneous symmetry breaking (16).

There are, however, interesting consequences of the interplay of topology and strong correlation, for example in frustrated quantum magnetism (17,18). For a sodium iridate, a correlated  $Z_2$  phase has been predicted (19,20). Also, the concept of a topological Mott insulator (21) has no analogue in band theory. These problems have been recently reviewed (22,23). Another issue is the stability of topologically protected phases towards electron correlation (22). It has been pointed out that strong electron correlation could increase the size of the inverted band gap (24) and ensure centering the gap about the Fermi energy.

As of today, there is no established correlated topological insulator but the candidate attracting most interest is the topological Kondo insulator (24,25). A Kondo insulator has a small band gap due to the Kondo effect, i. e., the hybridization of itinerant conduction electrons and localized f electrons. Dzero et al. realized that the odd parity of the f states

together with the even parity of d states fulfills the precondition for band inversion and ultimately a  $Z_2$  topological insulator phase (25). After the initial prediction of topological Kondo insulators and the finding that there are weak and strong topological insulator phases depending on the energetic alignment of the f level (25), it was found that due to the cubic symmetry of  $\text{SmB}_6$ , a weak topological insulator phase characterized by an even number of Dirac cones in the surface Brillouin zone does not exist leading to the prediction of a strong topological insulator for  $\text{SmB}_6$  (26). In calculations for the (100) surface of  $\text{SmB}_6$ , three independent theoretical approaches predicted an odd number of Dirac cone surface states per surface Brillouin zone as required for a strong topological insulator (26-28), see Fig. 1.

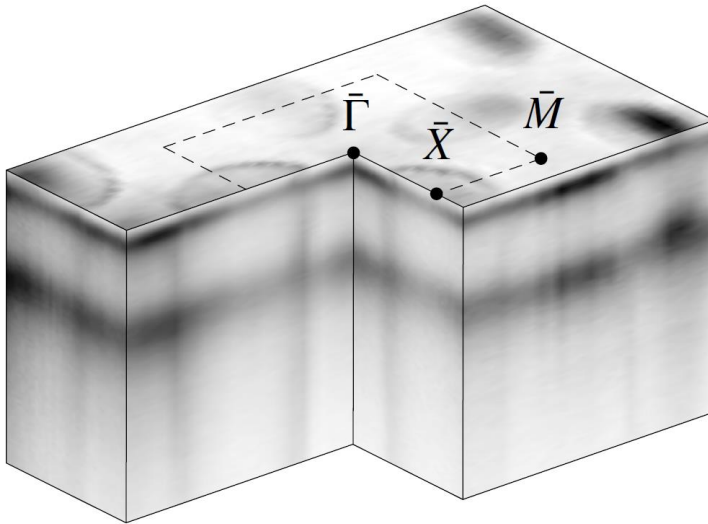


Fig. 1. ARPES data of the Fermi surface of  $\text{SmB}_6$  (100). Four Fermi surface ellipses appear centered at the  $\bar{X}$  point (two per surface Brillouin zone) and a surface state at the center  $\bar{\Gamma}$ . Similar data were reported by most ARPES studies of  $\text{SmB}_6$ . The present data were taken at 70 eV photon energy.

Several ARPES studies reported surface states of  $\text{SmB}_6$ . Neupane et al. (29) measured Fermi surface contours with 7 eV laser excitation. The symmetrized data showed elliptical contours around  $\bar{X}$  and finite ARPES intensity at  $\bar{\Gamma}$ . Frantzeskakis et al. (30) also measured

contours at  $\bar{X}$  and noted that the expected dispersion of a Dirac cone is not observed. They interpreted the contours at  $\bar{X}$  as showing a three-dimensional dispersion, different from most other studies. Jiang et al. (31) measured at low temperature and also observed the X contours. In addition, they show intensity at  $\bar{\Gamma}$ . They concluded that measurements with circularly polarized light confirm the expected spin texture of the contours at  $\bar{X}$  (31). A detailed investigation of the  $\bar{X}$  contours has been conducted by Denlinger et al. (32). Xu et al. (33) measured spin-resolved photoemission of the Fermi surface contours at  $\bar{X}$ . Their data supported the expected spin texture. Another confirmation of the contour at  $\bar{X}$  was published by Min et al. (34). The data are consistent in their observation of the contour at  $\bar{X}$  with the exception that Neupane et al. (29) reported a different size of the contour and not all studies report intensity at  $\bar{\Gamma}$ . In no case, a Dirac cone dispersion could be observed at  $\bar{\Gamma}$  or at  $\bar{X}$ .

We would like to discuss at first the surface state at  $\bar{\Gamma}$  and prerequisite for this discussion is the observation that cleaving of our SmB<sub>6</sub> crystals leads to two different terminations (35). Interestingly, core-level spectra of B 1s and Sm 4f show that these are chemically pure. Since the state at  $\bar{\Gamma}$  appears differently for the two terminations, this allowed us to observe the dispersion of the  $\bar{\Gamma}$  state in detail for the first time (35).

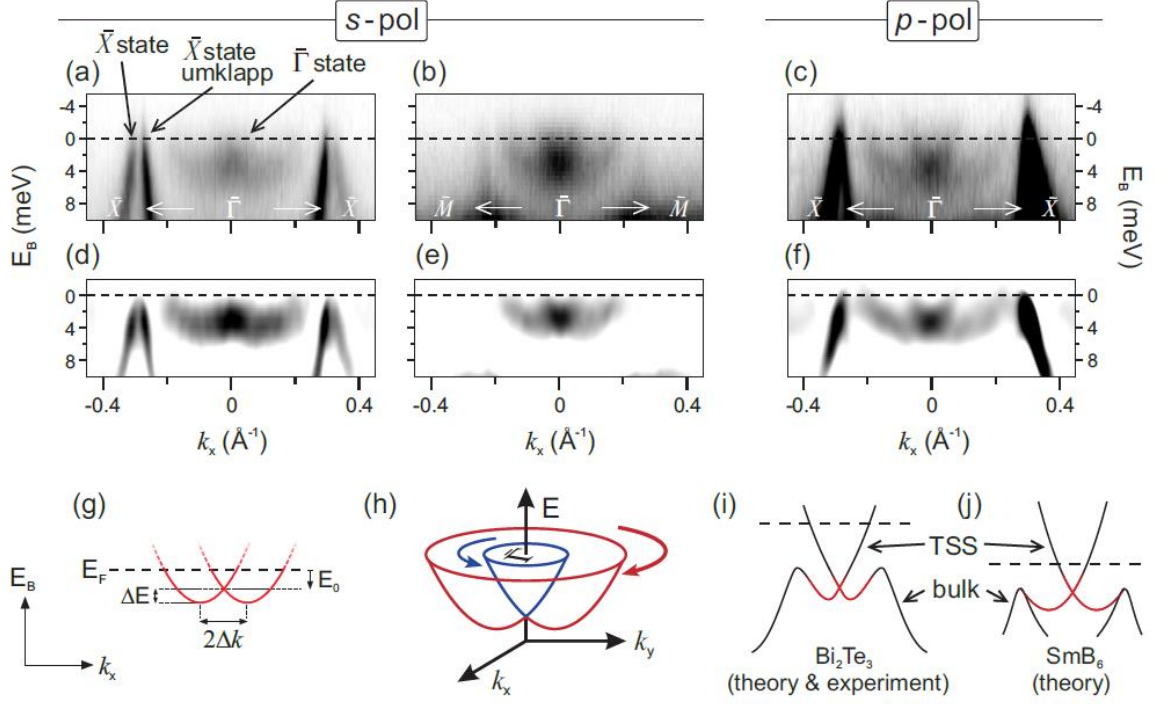


Fig. 2. ARPES study of the state at  $\bar{\Gamma}$ . All data show a Rashba splitting as sketched in (g, h). In cuts (a, c, d, f) also the elliptical Fermi surface contour at  $\bar{X}$  appears together with the  $\bar{\Gamma}$  state and together with an umklapp contour. A cut rotated by  $45^\circ$  (b, e) shows that the Rashba split bands are not connected to the valence band which would still enable a topological surface state in analogy to the case of the topological insulator  $\text{Bi}_2\text{Te}_3$  (i, j). The photon energy is 31 eV.

For the termination by Sm atoms, the state shows the dispersion of a massive particle (35). In principle, this could be a massive, i. e., gapped Dirac cone. However, for the termination by B atoms, the state shows a Rashba splitting (35). This is shown in Fig. 2 where the contour at  $\bar{X}$  appears together with the  $\bar{\Gamma}$  state. The elliptical contours at  $\bar{X}$  show an umklapp contour around  $\bar{\Gamma}$  which is labeled in Fig. 2a. This umklapp contour makes it difficult to judge whether there is a connection of the split surface state to the bulk valence band as it occurs for example with the Dirac cone surface state of the topological insulator  $\text{Bi}_2\text{Te}_3$ , see the sketch in Fig. 2i. For this reason, the measurement in Fig. 2b displays a

different cut by  $45^\circ$  which does not show the background intensity from the umklapp contours at  $\bar{X}$ . There is no downward dispersion.

The consequence of this result is that it is not possible anymore to reach an odd number of Dirac cones in the surface Brillouin zone. The contours shown in Fig. 1 show two ellipses at  $\bar{X}$  in the Brillouin zone, which is an even number. Hence, the observation of the Rashba splitting alone shows that an odd number of Dirac cones cannot be obtained, independently of whether or not these ellipses correspond to Dirac cones.

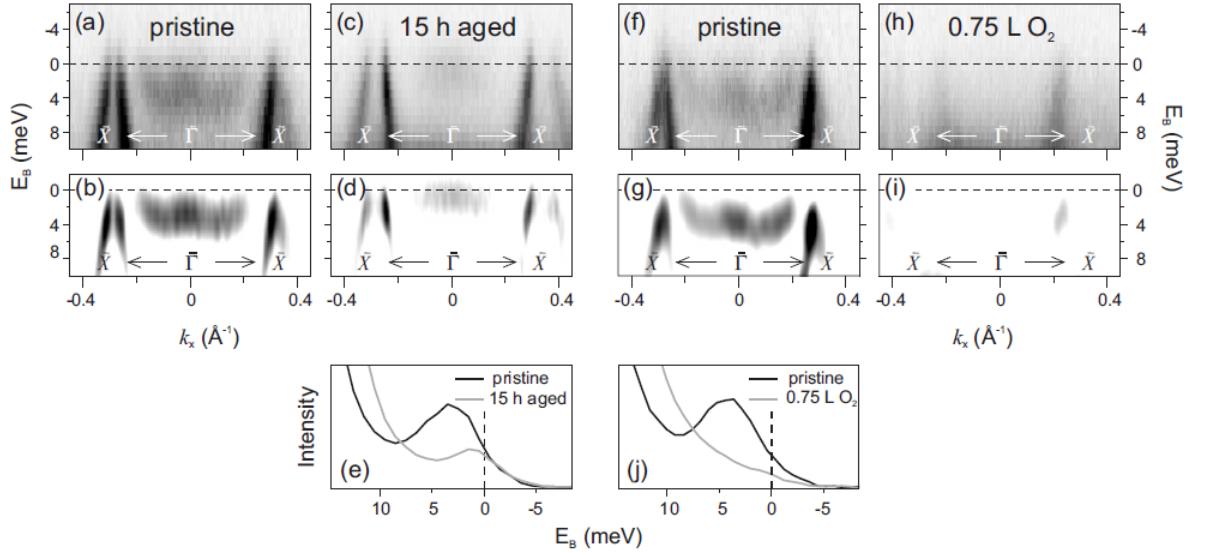


Fig. 3. Dependence of the Rashba-split surface state of B-terminated  $\text{SmB}_6$  on surface contamination. Absorption of residual gas (a-e) and molecular oxygen (f-j) lead to a decreasing photoemission intensity and disappearance of the surface state at  $\bar{\Gamma}$ .

Figure 3 shows the behavior of the Rashba-split surface state with contamination. In Fig. 3c, the sample is left for 15 h in the ultrahigh vacuum. The adsorption of residual gas leads to a diminished surface-state intensity. In Fig. 3f-j the experiment is repeated with controlled adsorption of 0.75 L oxygen. As a consequence, the surface state has completely disappeared because it has shifted above the Fermi level as Fig. 3j shows.

The Rashba splitting means that the surface states do not support a topological insulator assignment of  $\text{SmB}_6$ . Moreover, the sensitivity to contamination show that the surface state is not protected. These two observations independently indicate that the surface state at  $\bar{\Gamma}$  is trivial. Since the surface state has previously been used to confirm the nontrivial topology of  $\text{SmB}_6$ , the result means that ARPES data give no support for  $\text{SmB}_6$  as topological insulator (35). Since the cubic symmetry prohibits a weak topological insulator phase (26), the absence of the Dirac cone at  $\bar{\Gamma}$  would directly make  $\text{SmB}_6$  a trivial insulator. It is important to note that the present ARPES results are consistent with those of the literature. Also, in view of the present results, the fact that the state at  $\bar{\Gamma}$  is massive is visible is previous data by Xu et al. (36).

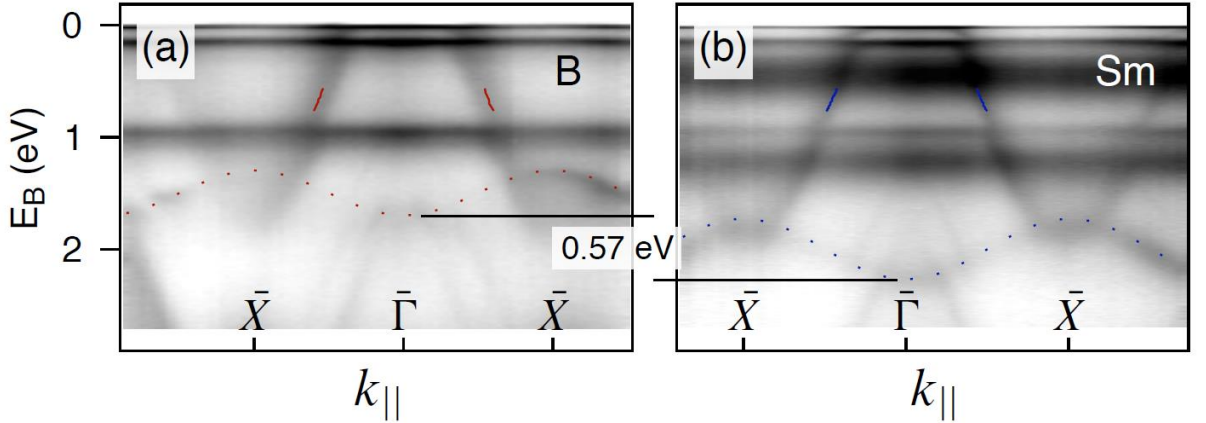


Fig. 4. Photoemission data of the region of the B 2p valence band. The shallow B 2p band marked with dots shifts by 0.57 eV depending on whether the termination is (a) B or (b) Sm. This shows that the surface potential depends strongly on the termination. A photon energy of 70 eV was used with p-polarization.

We want to discuss why the Rashba splitting appears only on the B terminated surface while the state forms a single parabola on the Sm terminated surface (35). Since the Rashba splitting depends on the gradient of the crystal potential perpendicular to the surface, this is in

principle supportive of the Rashba splitting.  $\text{SmB}_6$  is of CsCl structure and consequently the bulk truncated (100) surface would be highly polar. We observe chemically pure terminations based on core level spectra, supporting the bulk truncation model of the surfaces (35).

Therefore, different surface potential gradients are expected for the two terminations. There is another property of the Rashba effect that is important in this context: For a very large effective mass, a small Rashba parameter is sufficient for a large Rashba splitting in momentum space  $\Delta k_{\parallel}$ . Since the Rashba splitting is proportional to the effective mass

$$\Delta k_{\parallel} = m^* \alpha_R / \hbar^2 \quad (1)$$

the large effective mass of  $m^* \approx 17 m_e$  ( $m_e$  is the electron mass), which is the result of a strong 4f character, requires only a small parameter  $\alpha_R$  of  $(3.5 \pm 0.1) \times 10^{-12}$  eV m. The potential gradient as well as the spin-orbit interaction are included in the Rashba parameter. Figure 4 shows photoemission data of the region of the B 2p valence band which is marked with dots in the figure. It is seen that the position of the shallow B 2p band shifts by 0.57 eV depending on whether the surface is B or Sm terminated. This is strong support for the difference in surface potential gradient. It also contradicts the assumption by Zhu et al. (37) that the charge of the B surface layer is reduced with respect to the bulk.

In Fig. 5, we show that the Rashba splitting of  $\text{SmB}_6$  is of record size as compared to other surfaces. A large Rashba splitting in momentum space is important in spintronics since it determines the phase offset between spins and in this way the channel length in a spin field effect transistorsfor (46,47).

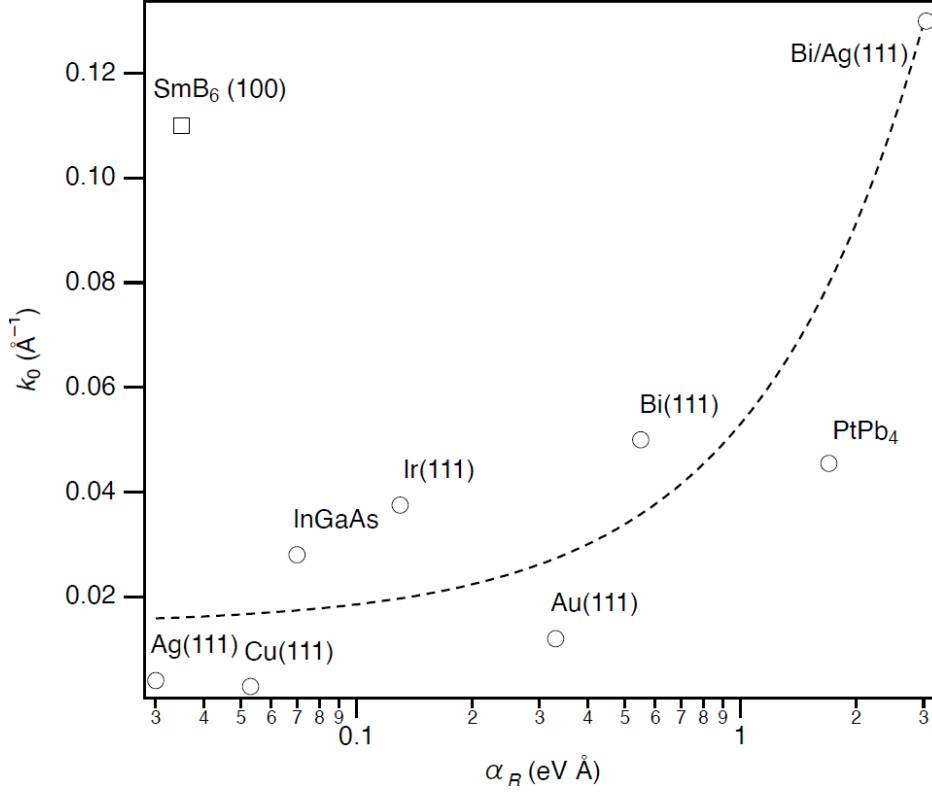


Fig. 5. Rashba splittings in momentum space for different systems. The case of SmB<sub>6</sub> is unique due to the strong 4f character and high effective mass. The data were taken from the following publications: PtPb<sub>4</sub> [38], Ag(111) [39], Cu(111) [40], (In,Ga)As [41], Ir(111) [42], Au(111) [43], Bi(111) [44], Bi/Ag(111) [45].

We want to discuss now the state at  $\bar{X}$  and the scenario underlying its appearance. First of all, the gap due to hybridization can be seen closing in in ARPES data when the temperature is increased. At first, bulk-induced ARPES intensity was observed above the Fermi level (32) and this was later confirmed (34,35). We have subsequently searched for changes in the valence band and could in this way identify both components of the split bulk band (35). Distinction between bulk and surface states was achieved by ageing and oxygen exposure. We observed two 5d-4f hybridized dispersions which are assigned to surface and bulk. For B termination, the surface 5d-4f hybrid is shifted by 10 meV to higher binding energy, and for Sm termination a similarly large shift occurs in the opposite direction, i. e., to lower binding energy. These small energy shifts of the order of 10 meV can occur below the

surface for both terminations. They are much smaller than the surface shifts of undercoordinated Sm which amount to about 0.3 eV. They are on the other hand much larger than the Kondo gap of  $\sim 3.5$  meV determined from the measured activation energy. Therefore, the 10 meV shift will render the surface metallic which explains the transport properties of SmB<sub>6</sub>. To show that this surface 5d-4f hybrid is not a state that exists only inside the bulk gap, photon-energy dependent dispersions were measured showing the two-dimensionality in a wide binding energy range (35). It is concluded that not only the surface state at  $\bar{\Gamma}$  is trivial, which is sufficient for the overall trivial character, but also at  $\bar{X}$ . Moreover, the surface state at  $\bar{X}$  explains the surface metallicity by a 10 meV energy shift.

It has previously been argued that there is an inconsistency between ARPES and scanning tunneling microscopy (STM) results (48). This appears to be the case when looking at the different terminations reported in our work and in the STM literature (49-52). To give an example, we observe exclusively two chemically pure surface terminations over the whole surface probed with an ARPES spot size of itself  $\sim 250$   $\mu\text{m}$  (Hla18). On the other hand, a  $(2 \times 1)$  reconstruction observed in STM is interpreted as a missing-row reconstruction (49,50). This is incompatible with our results since it requires the simultaneous presence of both undercoordinated B and undercoordinated Sm at the surface.

We have conducted a combined STM and ARPES experiment on the same samples and found that all cleaved surfaces fall into two categories. They are either  $(2 \times 1)$  with a peak at  $-7$  meV in scanning tunneling spectroscopy (STS) or  $(1 \times 1)$  where they show less sharp features (53). These STS spectra are very similar to those in the literature (49,50). For the  $(1 \times 1)$  surface this is also the case when comparing to previous STS work (49,50). The STS maximum is even more pronounced and can be located at  $-28$  meV (49). These energies correspond very well to the 10 meV binding energy shifts in two directions that we observe in ARPES where the terminations are identified directly based on the core-level spectra. For the

B terminated surface the binding energy is 27 meV, and for the Sm terminated surface it is 10 meV (35,53). Therefore, the STM results strongly support our conclusions that small binding energy shifts of 10 meV cause the surface metallicity of SmB<sub>6</sub>. The remaining disagreements with the STM literature are most likely due to the very small bias voltages employed previously (49-52). This is why a striking energy dependent contrast reversal (53) had remained undetected.

In summary, the Rashba splitting in SmB<sub>6</sub> is important in two ways. Due to the very large effective mass of  $\sim 17 m_e$  because of strong 4f character, it has one of the largest momentum offsets observed among Rashba split surface states. At the same time, its Rashba parameter including the potential gradient and the spin-orbit coupling, is by two orders of magnitude smaller. Secondly, the Rashba splitting, which would not have been observable in the experiment were the effective mass smaller, is essential to characterize the surface electronic structure as trivial. This insight from the delicate  $\bar{\Gamma}$  surface state prompted a more profound search for the origin of the robust surface metallicity of SmB<sub>6</sub> which was found in small energy shifts of 10 meV of the 5d-4f hybrid at  $\bar{X}$ . We caution, however, that our conclusions are based only on the surface states visible so far in ARPES and do not exclude topological surface states buried possibly underneath the surface

#### Acknowledgements

This work was supported by the Deutsche Forschungsgemeinschaft (SPP 1666). J. S.-B. acknowledges financial support from the Impuls- und Vernetzungsfonds der Helmholtz-Gemeinschaft under grant No. HRSF-0067.

#### References

- 1 E. I. Rashba, J. Supercond. Nov. Magn. 16, 599 (2003).

- 2 E. I. Rashba, V. I. Sheka, *Fizika tverd. tela. Collected Papers* 2, 162 (1959).  
Translation in the supplementary material of G. Bihlmayer, O. Rader, R. Winkler, *New J. Phys.* 17, 050202 (2015).
- 3 G. Dresselhaus, *Phys. Rev.* 100, 580 (1955).
- 4 Yu. A. Bychkov, E. I. Rashba, *JETP Lett.* 39, 78 (1984).
- 5 A. Manchon, H. C. Koo, J. Nitta, S. M. Frolov, R. A. Duine, *Nat. Mater.* 14, 871 (2015).
- 6 G. Bihlmayer, O. Rader, R. Winkler, Focus on the Rashba effect, *New J. Phys.* 17, 050202 (2015).
- 7 H. W. Yeom, M. Grioni, (eds.), Special issue on electron spectroscopy for Rashba spin-orbit interaction, *J. El. Spectr. Relat. Phenom.* 201, 2 (2015).
- 8 M. Z. Hasan, C. L. Kane, *Rev. Mod. Phys.* 82, 3045 (2010).
- 9 X.-L. Qi, S.-C. Zhang, *Rev. Mod. Phys.* 83, 1057 (2010).
- 10 B. A. Volkov, O. A. Pankratov, *JETP Lett.* 42, 178 (1985).
- 11 M. König, S. Wiedmann, C. Brüne, A. Roth, H. Buhmann, L. W. Molenkamp, X.-L. Qi, S.-C. Zhang, *Science* 318, 766 (2007).
- 12 C.-Z. Chang, J. Zhang, X. Feng, J. Shen, Z. Zhang, M. Guo, K. Li, Y. Ou, P. Wei, L. Wang, and Z. Q. Ji, *Science* 340, 167 (2013).
- 13 C. L. Kane, E. J. Mele, *Phys. Rev. Lett.* 95, 226801 (2005).
- 14 M. Gmitra, S. Konschuh, C. Ertler, C. Ambrosch-Draxl, J. Fabian, *Phys. Rev. B* 80, 235431 (2009).
- 15 D. Marchenko, A. Varykhalov, M. R. Scholz, G. Bihlmayer, E. I. Rashba, A. Rybkin, A. M. Shikin, O. Rader, *Nat. Commun.* 3, 1232 (2012).
- 16 V. Ginzburg, L. Landau, *Zh. Eksp. Teor. Fiz.* 20, 1064 (1950).
- 17 L. Balents, *Nature* 464, 199 (2010).
- 18 J. Reuther, R. Thomale, S. Rachel, *Phys. Rev. B* 86, 155127 (2012).

- 19 G. Jackeli, G. Khaliullin, *Phys. Rev. Lett.* 102, 017205 (2009).
- 20 A. Shitade, H. Katsura, J. Kunes, X. L. Qi, S. C. Zhang, N. Nagaosa, *Phys. Rev. Lett.* 102, 256403 (2009).
- 21 D. A. Pesin, L. Balents, *Nat. Phys.* 6, 376 (2010).
- 22 S. Rachel, *Rep. Prog. Phys.* 81, 116501 (2018).
- 23 M. Hohenadler, F. F. Assaad, *J. Phys.: Condens. Matter* 25, 143201 (2013).
- 24 M. Dzero, V. Galitski, *J. Exp. Theor. Phys.* 117, 499 (2013).
- 25 M. Dzero, K. Sun, V. Galitski, P. Coleman, *Phys. Rev. Lett.* 104, 106408 (2010).
- 26 V. Alexandrov, M. Dzero, and P. Coleman, *Phys. Rev. Lett.* 111, 226403 (2013).
- 27 T. Takimoto, *J. Phys. Soc. Jpn.* 80, 123710 (2011).
- 28 F. Lu, J. Zhao, H. Weng, Z. Fang, and X. Dai, *Phys. Rev. Lett.* 110, 096401 (2013).
- 29 M. Neupane, N. Alidoust, S.-Y. Xu, T. Kondo, Y. Ishida, D.-J. Kim, C. Liu, I. Belopolski, Y. J. Jo, T.-R. Chang, H.-T. Jeng, T. Durakiewicz, L. Balicas, H. Lin, A. Bansil, S. Shin, Z. Fisk, and M. Z. Hasan, *Nat. Commun.* 4, 2991 (2013).
- 30 E. Frantzeskakis, N. de Jong, B. Zwartsenberg, Y. K. Huang, Y. Pan, X. Zhang, J. X. Zhang, F. X. Zhang, L. H. Bao, O. Tegus, A. Varykhalov, A. de Visser, M. S. Golden, *Phys. Rev. X* 3, 041024 (2013).
- 31 J. Jiang, S. Li, T. Zhang, Z. Sun, F. Chen, Z. R. Ye, M. Xu, Q. Q. Ge, S. Y. Tan, X. H. Niu, M. Xia, B. P. Xie, Y. F. X. H. Chen, H. H. Wen, and D. L. Feng, *Nat. Commun.* 4, 3010 (2013)
- 32 J. D. Denlinger, J. W. Allen, J.-S. Kang, K. Sun, J. W. Kim, J. H. Shim, B.-I. Min, D. J. Kim, and Z. Fisk, *arXiv* (2013), 1312.6637v1.
- 33 N. Xu, P. K. Biswas, J. H. Dil, R. S. Dhaka, G. Landolt, S. Muff, C. E. Matt, X. Shi, N. C. Plumb, M. Radovic, E. Pomjakushina, K. Conder, A. Amato, S. V. Borisenko, R. Yu, H. Weng, Z. Fang, X. Dai, J. Mesot, H. Ding, M. Shi, *Nat. Commun.* 5, 4566 (2014).

- 34 C.-H. Min, P. Lutz, S. Fiedler, B. Y. Kang, B. K. Cho, H. D. Kim, H. Bentmann, and F. Reinert, *Phys. Rev. Lett.* 112, 226402 (2014).
- 35 P. Hlawenka, K. Siemensmeyer, E. Weschke, A. Varykhalov, J. Sánchez-Barriga, N. Y. Shitsevalova, A. V. Dukhnenko, V. B. Filipov, S. Gabáni, K. Flachbart, O. Rader, E. D. L. Rienks, *Nat. Commun.* 9, 517 (2018).
- 36 N. Xu, X. Shi, P. K. Biswas, C. E. Matt, R. S. Dhaka, Y. K. Huang, N. C. Plumb, M. Radovic, J. H. Dil, E. Pomjakushina, K. Conder, A. Amato, Z. Salman, D. M. Paul, J. Mesot, H. Ding, M. Shi, *Phys. Rev. B* 88, 121102 (2013).
- 37 Z.-H. Zhu, A. Nicolaou, G. Levy, N. P. Butch, P. Syers, X. F. Wang, J. Paglione, G. A. Sawatzky, I. S. Elfimov, and A. Damascelli, *Phys. Rev. Lett.* 111, 216402 (2013).
- 38 K. Lee, D. Mou, N. H. Jo, Y. Wu, B. Schrunk, J. M. Wilde, A. Kreyssig, A. Estry, S. L. Bud'ko, M. C. Nguyen, L.-L. Wang, C.-Z. Wang, K.-M. Ho, P. C. Canfield and A. Kaminski, *Phys. Rev. B* 103, 085125 (2021).
- 39 D. Popović, F. Reinert, S. Hüfner, V. G. Grigoryan, M. Springborg, H. Cercellier, Y. Fagot-Revurat, B. Kierren, and D. Malterre, *Phys. Rev. B* 72, 045419 (2005).
- 40 A. Tamai, W. Meevasana, P. D. C. King, C. W. Nicholson, A. de la Torre, E. Rozbicki, and F. Baumberger, *Phys. Rev. B* 87, 075113 (2013).
- 41 J. Nitta, T. Akazaki, H. Takayanagi, and T. Enoki, *Phys. Rev. Lett.* 78, 1335 (1997).
- 42 A. Varykhalov, D. Marchenko, M. R. Scholz, E. D. L. Rienks, T. K. Kim, G. Bihlmayer, J. Sánchez-Barriga and O. Rader, *Phys. Rev. Lett.* 108, 066804 (2012).
- 43 S. LaShell, B. A. McDougall, and E. Jensen, *Phys. Rev. Lett.* 77, 3419 (1996).
- 44 Y. M. Koroteev, G. Bihlmayer, J. E. Gayone, E. V. Chulkov, S. Blügel, P.M. Echenique, and P. Hofmann, *Phys. Rev. Lett.* 93, 046403 (2004).
- 45 C. R. Ast, J. Henk, A. Ernst, L. Moreschini, M. C. Falub, D. Pacilé, P. Bruno, K. Kern and M. Grioni, *Phys. Rev. Lett.* 98, 186807 (2007).
- 46 S. Datta and B. Das, *Appl. Phys. Lett.* 56, 665 (1990).

- 47 Q. Liu, Y. Guo, and A. J. Freeman, *Nano Lett.* 13, 5264 (2013).
- 48 J. W. Allen, *Philos. Mag.* 96, 3227 (2016).
- 49 M. M. Yee, Y. He, A. Soumyanarayanan, D.-J. Kim, Z. Fisk, J. E. Hoffman, arXiv:1308.1085, 2013.
- 50 S. Rößler, T. H. Jang, D.-J. Kim, L. H. Tjeng, Z. Fisk, F. Steglich, S. Wirth, *Proc. Natl. Acad. Sci. USA* 111, 4798 (2014).
- 51 W. Ruan, C. Ye, M. Guo, F. Chen, X. Chen, G.-M. Zhang, Y. Wang, *Phys. Rev. Lett.* 112, 136401 (2014).
- 52 Z. Sun, A. Maldonado, W. S. Paz, D. S. Inosov, A. P. Schnyder, J. J. Palacios, N. Y. Shitsevalova, V. B. Filipov, P. Wahl, *Phys. Rev. B* 2018, 97, 235107.
- 53 H. Herrmann, P. Hlawenka, K. Siemensmeyer, E. Weschke, J. Sánchez-Barriga, A. Varykhalov, N. Y. Shitsevalova, A. V. Dukhnenko, V. B. Filipov, S. Gabáni, K. Flachbart, O. Rader, M. Sterrer, E. D. L. Rienks, *Adv. Mater.* 29, 1906725 (2020).